J Therm Anal Calorim (2009) 98:125–131
DOI 10.1007/s10973-009-0227-9

Influence of sodium chloride on the melting of ice and crystallization and dissociation of CCl_3F hydrate in water in oil emulsion

L. Komunjer · M. Ollivon · B. Fouconnier · A-T Luong · I. Pezron · D. Clausse

Special Chapter dedicated to the memory of dr. Michel Ollivon

Abstract Trichlorofluoromethane (CCl_3F) and water form clathrate hydrate which melts at 8.5 °C under atmospheric pressure. By DSC and X rays analysis we could distinguish between hydrate and ice formed in emulsion containing NaCl and show that quantity of hydrate formed and its dissociation temperature are dependent on solution concentration. The equilibrium curve hydrate-NaCl solution is displaced towards higher temperatures with respect to corresponding ice curve. Consequently solid–liquid equilibrium can not be established in presence of both solids. Growth of hydrate crystals at the expense of ice was evidenced. Role of salt in hydrate growth and ice melting is examined.

Keywords Clathrate hydrate · CCl_3F · Ice · NaCl · Water-in-oil emulsion · XR-DSC analysis

Introduction

This article is dedicated to the memory of Michel Ollivon whose contribution was essential in the understanding of the formation of hydrate in the emulsions thanks to the combined DSC/X-Rays technique he developed. The results described in this article were obtained with his full contribution.

L. Komunjer (✉) · B. Fouconnier · A.-T. Luong · I. Pezron · D. Clausse
Département de Génie des Procédés Industriels, Université de Technologie de Compiègne, 60205 Compiègne, France
e-mail: komunjer@utc.fr

M. Ollivon
Laboratoire Physico-Chimie des Systèmes Polyphasés, Université Paris XI, Châtenay-Malabry, France

Hydrate of trichlorofluoromethane (CCl_3F) can be classified among gas hydrates similar to natural gas clathrates although highly volatile CCl_3F is in liquid state when it reacts with water to give the corresponding solid hydrate. Nevertheless, similarly to the well known tetrahydrofuran (THF) clathrate hydrate [1], it was considered as convenient model system [2, 3] to study the creation of solid plugs in crude oil or natural gas off-shore installations because it can be formed at 8 °C at atmospheric pressure while gas hydrates such as methane hydrate need low temperature and high pressure conditions [4–8]. In addition, CCl_3F clathrate hydrate presents the same crystal structure, so-called structure II, as natural gas hydrate. Formation of hydrate plugs can be of great danger in terms of security and production cost. Namely, crystallization of solid hydrate inside a pipe-line might cause significant production slowdown and/or require costly heating-up procedures. Furthermore, presence of salty water, crude oil and naturally occurring surface active compounds such as asphaltenes gives rise to the formation of emulsions, often of water in oil type [5, 9]. Due to the high total surface area of contact, the exchange between the structure forming water molecules and the host molecules present in the oil phase is favored at the oil–water interface. Therefore it seems necessary to study the mechanism of formation of hydrates in water in oil emulsion containing dissolved NaCl in the water droplets.

Previous works concerning the formation of CCl_3F hydrate within water in oil emulsions evidenced significant delay in the formation of the solid hydrate. Namely, for agitated emulsions with volume of about 200 mL the delay of few degrees was reported [2]. For non agitated emulsion sample of few mm^3 much more important delay is observed when the emulsion is regularly cooled down to −50 °C [3, 10]. During cooling at 2 K/min only formation

of ice is detected at about −40 °C as might be expected for water in oil emulsion without CCl_3F [11–14]. Thanks to the use of the coupled technique DSC/X-rays [10], it was found that hydrate forms during the progressive melting of ice which is caused by the presence of NaCl within droplets. In addition, by using DSC alone the dissociation energy of the hydrate as a function of temperature could be deduced by varying the concentration and nature of salt. It was shown also that, with respect to solid hydrate, the presence of salts has a similar effect as it has on the melting of ice in frozen solutions [15].

In this article, the results on water in oil emulsions containing NaCl and obtained by coupling DSC and X-rays are reported. The phenomena studied concern the melting of water in oil emulsions containing CCl_3F in the oil phase that have been quenched in liquid nitrogen before heating. The behavior of the solid phases formed by quenching is examined between −25 °C and +20 °C.

Materials and methods

Concentrated water in oil emulsions studied here are of dispersed phase volume fraction 0.60. Emulsion is prepared at room temperature by introducing aqueous solution of sodium chloride (purity of NaCl >99.5%) into aliphatic hydrocarbon oil Exxol D80 (Exon Mobil Chemicals) containing 4% v/v of non-ionic surfactant tetraoxyethylene nonyl phenyl ether (Berol 26). Emulsification is performed by means of Polytron PT 3100 (Kinematica AG, Swisse) at 10,000 rpm during 10 min. Hydrate forming substance used is trichlorofluoromethane CCl_3F of purity >99.5%. It is liquid at room temperature but highly volatile (ebullition temperature 24 °C at normal pressure). In order to minimize evaporation of CCl_3F it is introduced in an emulsion prepared in advance and kept at 4 °C. The quantity of CCl_3F to introduce into emulsion is calculated by assuming 17 water molecules of water present in dispersed phase for each molecule of CCl_3F incorporated into oil phase. The volume of the oil phase is reduced accordingly in order to keep the emulsion volume fraction of 0.60 constant.

Aqueous salt solutions are prepared with de-mineralized water (conductivity 0.6 μS/cm). All chemical are purchased from Sigma Aldrich, France and used as received.

Small quantity of emulsion (of order of 20 mg) is introduced into a capillary of diameter 1.5 mm (Glass W. Miller, Berlin, Germany). Rapid crystallization of the sample is subsequently provoked by placing the capillary into liquid nitrogen bath prior to introduction into sample holder of the X-rays diffraction as function of temperature (XRDT) apparatus preconditioned to approximately −25 °C. The XRDT set-up was installed on line D22 of LURE synchrotron source. Detailed description of apparatus can be found in references [16, 17]. Both, heat flow and structural information are collected on the same emulsion sample. During heating programmed at 1 K/min X-rays diffraction data are collected during 58 s (2 s are allowed for saving the file and restarting new measurement) while heath flow is monitored continuously. Conversion of channel to angle of diffraction is performed by means of calibration curves obtained with known substances, tristearate and hexagonal ice. For details see references [10, 17].

Crystal structure of solid hydrate depends on the nature of enclathrated gas [18]. Two different cubic forms are known: structure I with cell parameter $a = 12$ Å containing 8 cavities made of 46 water molecules and structure II with $a = 17.3$ Å [17] containing 8 large and 16 small cavities and 136 water molecules. If only large cavities are occupied by gas molecules it means that structure II clathrate hydrate contains 136/8 i.e. 17 water molecules for each gas molecule. For smaller gas species the minimum hydration number is 136/24 i.e. 5.67. These clathrate structures are therefore non-stoechiometric compounds. Small gas molecules, such as methane, are known to form cubic structure I while molecules with larger van der Waals diameter, such as CCl_3F, or mixtures of two different gas molecules form face centered cubic structure II [19, 20]. Unfortunately, no data for atomic positions in structure II CCl_3F hydrate is available in the literature. However, for identification purposes the positions of diffraction lines of other known structure II hydrates can be used since slight differences of lattice parameter a observed for gas molecules of different sizes [20] remain negligible. The same is true for effect of temperature at which structural analysis is performed [21].

Crystallographic data used for identification of the solid phase are presented in Table 1.

Results and discussion

Owing to the high amount of energy involved in crystallization and melting of water experimental evidence of solid hydrate formation should be achievable by calorimetric measurements. Nonetheless, this technique alone does not allow the discrimination between ice and clathrate hydrate since in both cases the energy liberated or absorbed

Table 1 2θ values for hexagonal ice [10] and structure II clathrate hydrate [20]

Solid	Position of diffraction line 2θ (°)					
Ice	22.7	24.2	25.8			
Hydrate	17.0	17.7	20.5	22.3	25.2	26.7

Diffraction patterns corresponding to NaCl or $NaCl{\cdot}2H_2O$ were not observed under the experimental conditions of the present study

is mainly due to hydrogen bonds between water molecules [19]. Simultaneous presence of ice and hydrate, often signaled in scientific reports [1, 3, 10, 22] and in field records, can render the data analysis rather complicated. Debenedetti's group calorimetric study [23] evidenced coexistence of ice and clathrate hydrate in water in oil emulsions. They examined the mechanism of nucleation of solid phase and showed that ice is good nucleating agent for hydrate but hydrate is not good nucleation support for ice. In a recent study dealing with formation of gas hydrate in water in crude oil emulsions Davies et al. [22] show that nucleation of gas hydrate and of ice are intimately related but the exact mechanism could not be provided. In our earlier study on water in oil emulsion containing 3%NaCl we have arrived to similar conclusion [3, 10].

Nucleation and growth of ice crystals in dispersed water droplets is known to take place at large degrees of undercooling of order of 40 K during steady cooling experiments on water in oil emulsions [24–26]. Furthermore, in presence of salts inducing the well known cryoscopy effect, even further decrease of the temperature of solidification is observed [27]. Similar effect, also known as thermodynamic inhibition effect of solutes is sometimes exploited in order to restrain the formation of solid hydrate in pipelines. Nevertheless, the important quantity of substances used and environmental concerns are fueling research for other less harmful solutions such as so-called kinetic inhibitors which should slow-down the nucleation and/or growth of clathrate hydrate. It is therefore obvious that the mechanisms involved in those processes should be elucidated and in particular the possible role ice and presence of salt might play in the process.

In order to interpret the acquired experimental data the phase diagrams are needed. Although the one corresponding to water + NaCl with eutectic point at −21.6 °C is well known one important feature should be added here, namely the existence of another eutectic point noted E2 (Fig. 1). It was first detected as metastable eutectic melting at −27 °C by Kanno and Angel [28] but no precision concerning the composition was given at that time. Clausse et al. [27] confirmed the existence of this transition and proposed the interpretation as indicated in Fig. 1: the eutectic melting peak at −27 °C corresponds to the metastable mixture of anhydrous NaCl and ice in emulsion droplets. The possible transition from metastable anhydrous NaCl to stable $NaCl{\cdot}2H_2O$ has not been proved yet.

Concerning the hydrate-NaCl phase diagram, it is much less known because its experimental determination is not straightforward. It has been obtained by performing DSC experiments on water in oil emulsions with CCl_3F present in the oil phase and with different kind of salts dissolved in the water droplets [15]. From the dissociation temperatures of the hydrate in equilibrium with the solutions and by

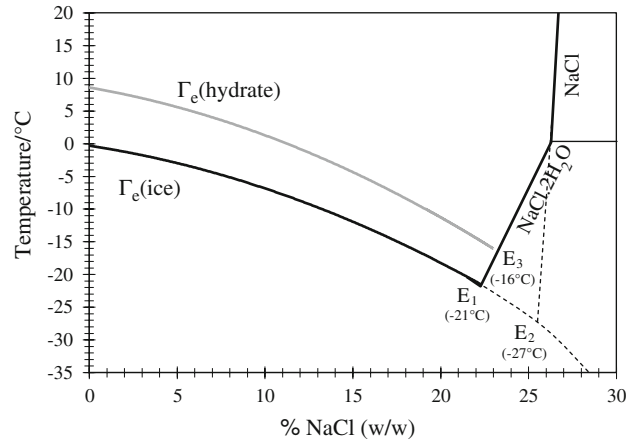

Fig. 1 Pseudo-phase diagram of a H_2O/NaCl solution with CCl_3F present in the continuous oil phase of emulsion. Γ_e(hydrate): coexistence of hydrate and aqueous salt solution as a function of salt concentration [15]; Γ_e(ice): Equilibrium curve for ice and aqueous salt solution: E1: eutectic point ice-$NaCl{\cdot}2H_2O$; E2: eutectic point ice-NaCl [27]; E3: intersection of equilibrium curves hydrate-NaCl solution and $NaCl{\cdot}2H_2O$-solution

using a thermodynamic approach the equilibrium points and the dissociation energy have been obtained. The equilibrium curves corresponding to ice and hydrate are drawn on the same diagram of Fig. 1 for comparison purposes. Referring to water + NaCl diagram, the known eutectic point at −21.6 °C related to $NaCl{\cdot}2H_2O$ is noted E1. The eutectic related to the anhydrous salt is also indicated and noted E2. Point E3 at approximately −16 °C refers to the intersection of two equilibrium curves: the one corresponding to the equilibrium between solid hydrate and aqueous solution of NaCl and the other to the solubility curve of $NaCl{\cdot}2H_2O$ in water. This point could be considered as the eutectic mixture composed of aqueous salt solution, solid hydrate and solid $NaCl{\cdot}2H_2O$.

For emulsion containing aqueous solution with 1%NaCl, the X Rays patterns alone are shown in Fig. 2.

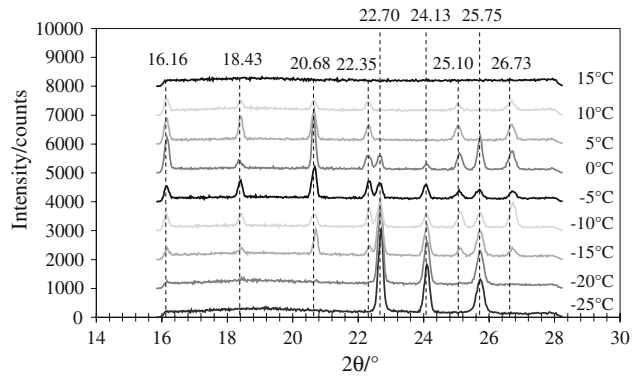

Fig. 2 Evolution of X-rays diffractograms during heating from −25 °C to +15 °C at 1 °C/min of an emulsion containing 1%NaCl in dispersed phase

At temperature of −25 °C one can observe clear-cut pattern of hexagonal ice characterised by lines at positions given in Table 1. The intensity of these lines decreases during heating as can be expected due to the progressive melting of ice in presence of salt. In addition, new lines start appearing; their positions are characteristic of gas hydrate structure II given in Table 1. During heating the intensity of hydrate lines first increases steadily then varies strongly between −10 °C and +10 °C to disappear afterwards. Intensity of ice lines diminishes strongly until approximately 0 °C in rather good agreement with the ice melting point for this concentration: $T_e = -1$ °C (Fig. 1). These results show that hydrate forms during the progressive melting of ice and dissociates when ice is no longer present in the droplets.

According to the equilibrium curve referred to as Γ_e hydrate of Fig. 1, the aqueous 1%NaCl solution and solid CCl_3F hydrate can coexist until approximately +8 °C; at +8 °C all solid hydrate should be dissociated and give place to the initial solution dispersed as emulsion drops. This is exactly what is observed on the Fig. 3 representing the calorimetric signal together with intensities of different X ray lines.

Heat flow signal shows melting of ice-salt eutectic at about −22 °C, one small endothermic signal at about −16 °C followed by progressive melting of ice followed by a large double peak between −15 °C and +10 °C. The last one of the two peaks, the apex at around 8.5 °C can be attributed to the dissociation of solid hydrate. Due to the rather low scanning rate employed this temperature corresponds well to the equilibrium value given by curve Γ_e hydrate of Fig. 1. The precise determination of this equilibrium temperature, which needs a well defined eutectic point, is developed elsewhere [29].

The signal with the apex at about +1 °C is probably a superposition of the exothermic signal due to the formation

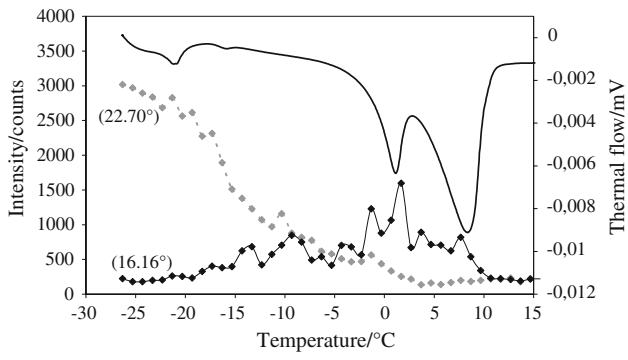

Fig. 3 Heating at 1 °C/min from −25 °C to +15 °C of an emulsion containing an aqueous solution of 1%NaCl; *continuous dark line* calorimetric signal, *black dots and lines* intensity of gas hydrate line (16.16 °), *grey lines and dots* intensity of hexagonal ice (22.70 °)

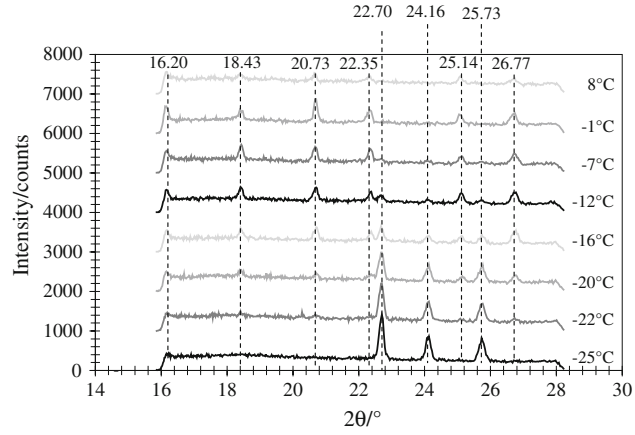

Fig. 4 Evolution of X-rays diffractograms recorded during heating from −25 °C to +15 °C at 1 °C/min of an emulsion containing 3%NaCl

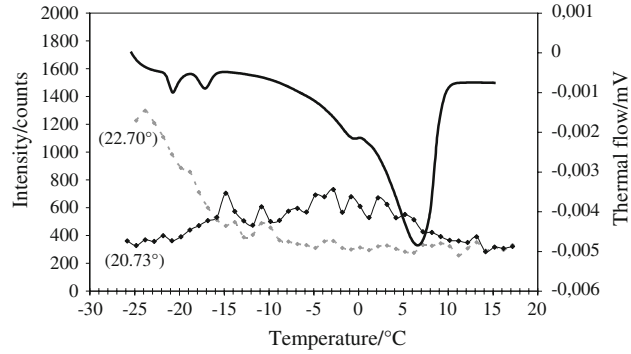

Fig. 5 Heating at 1 °C/min from −25 °C to +15 °C of an emulsion containing an aqueous solution of 3%NaCl; *continuous black line* calorimetric signal; *black dots and lines* intensity of gas hydrate line (20.73 °); *grey lines and dots* intensity of hexagonal ice (22.70 °)

of hydrate and the endothermic signal due to the melting of ice. The selected lines corresponding to ice and hydrate shown in Fig. 3 confirm this interpretation.

The results obtained by increasing the NaCl concentration to 3%, are given on Figs. 4 and 5.

One can note that the evolution of the X rays is similar to the one observed for 1%NaCl with one important exception: the intensity of diffraction signal is much lower: maximum intensity was over 3,000 counts for 1%NaCl and it is only about 1,000 counts for 3%NaCl. Diffracted intensity can be considered as an indicator of the quantity of crystalline phase present in solidified emulsion. From −22 °C the intensity of ice lines decreases in the same manner as in case of 1%NaCl. One can observe that the decrease of intensity of ice lines and increase of lines characteristic of gas hydrate coincide. Maximal intensity of hydrate lines coincides with the background level of ice lines intensity. One can also note that the decrease of ice lines intensity is even steeper comparing to the 1%NaCl

case Furthermore it seems that ice begins to melt before the well known eutectic point at −21.6 °C. This phenomenon can be attributed to the melting of the anhydrous eutectic situated at −27 °C (E2 in Fig. 1). The existence of this eutectic could explain the very first signs of gas hydrate line at 2θ of 20.7 ° which appears and increases in intensity already from −25 °C.

Calorimetric signal shows two endothermic events: one peak due to the eutectic melting of ice at about −21 °C and another similar signal at about −16 °C, temperature which is very near of the one corresponding to point E3 of Fig. 1. The well defined signal with apex at +7 °C is attributed to the dissociation of the hydrate in agreement with the hydrate equilibrium curve.

The results of X rays analysis obtained with solutions containing 10%NaCl are presented in Figs. 6 and 7.

The following phenomena are observed: between −25 °C and −15 °C the ice lines strongly decrease in intensity while those of gas hydrate increase. As previously indicated, the first signs of diffraction lines characteristic of structure II hydrate are visible at temperature of −23 °C; at the same time the intensity of ice lines decrease. The proposed interpretation is analogous to the one given for the 3%, namely as the result of the formation of hydrate due to the anhydrous eutectic melting. Comparing to the lower concentrations of NaCl the signal of eutectic melting visible at approximately −22 °C is energetically more important. It is followed by another endothermic signal situated at around −15 °C which can be attributed to hydrate NaCl eutectic. It is similar to the signal observed also at 3%NaCl but energetically more important since the concentration of salt in solution is higher. The last signal at about +1 °C is attributed to the hydrate dissociation in agreement with the hydrate equilibrium curve of Fig. 1.

By increasing the salt concentration to 20%NaCl, results presented in Figs. 8 and 9, the tendency observed at lower NaCl concentration is confirmed: on one hand the diffracted intensity is much weaker for all observed lines; on the other hand the melting peaks are situated at lower temperatures.

From the very beginning of heating i.e. from −25 °C the intensity of ice line decreases rapidly and gets to the

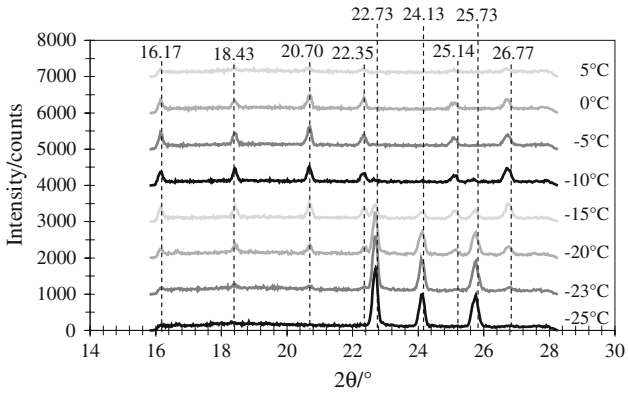

Fig. 6 Evolution of diffractograms recorded during heating from −25 °C to +15 °C at 1 °C/min of an emulsion containing 10%NaCl

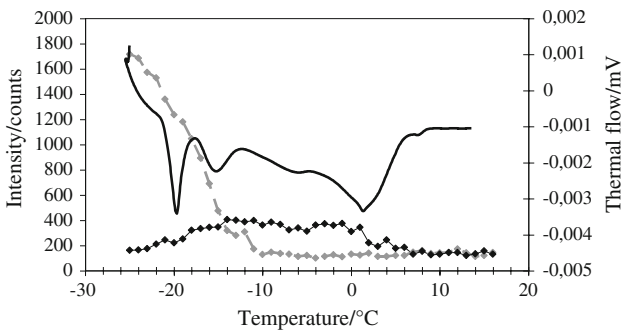

Fig. 7 Heating at 1 °C/min from −25 °C to +15 °C of an emulsion containing an aqueous solution of 10%NaCl; *continuous black line* calorimetric signal, *black dots and lines* intensity of gas hydrate line (16.17°), *grey lines and dots* intensity of hexagonal ice (22.70°)

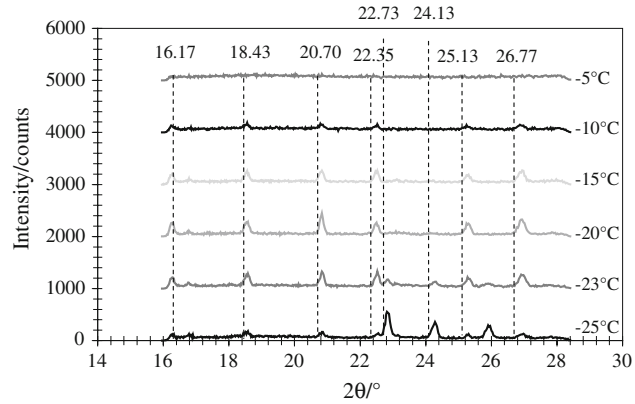

Fig. 8 Evolution of diffractograms recorded during heating from −25 °C to +15 °C at 1 °C/min of an emulsion containing 20%NaCl

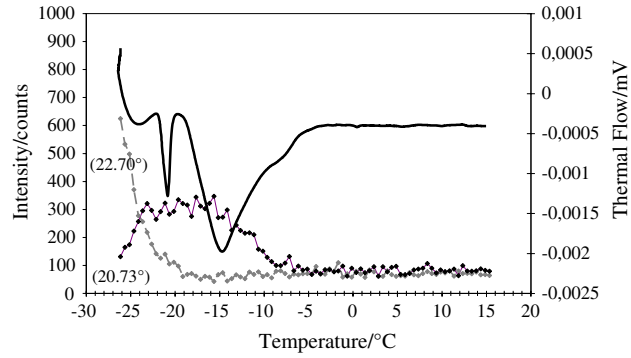

Fig. 9 Heating at 1 °C/min from −25 °C to +15 °C of an emulsion containing an aqueous solution of 20%NaCl; *continuous black line* calorimetric signal, *black dots and lines* intensity of gas hydrate line (20.73°), *grey lines and dots* intensity of hexagonal ice (22.70°)

background noise level already at −20 °C. This observation further corroborates the hypothesis of eutectic melting from −27 °C as indicated earlier. Gas hydrate line remains at its maximum intensity between −23 °C and −15 °C and gets to the background noise level between −10 and −5 °C. Another interesting observation is the confirmation of the presence of lines characteristic of gas hydrate from the very beginning of the experiment (diffractogram detected at −25 °C shown in Fig. 8) i.e. well before eutectic point at −21.6 °C in accordance with the existence of metastable anhydrous NaCl eutectic point at −27 °C.

In Fig. 9 one energetically important signal of eutectic melting of ice can be observed at −22 °C; it is accompanied by very rapid fall of ice lines intensity while gas hydrate lines remain at their maximum level. One can verify that ice diffraction lines are no longer visible already at −20 °C which is in reasonable agreement with the ice melting point for this concentration, namely—18 °C (see Fig. 1).

The signal between approximately −17 °C and −5 °C might represent the convolution of several phenomena: hydrate eutectic melting, progressive ice melting and formation and eventually dissociation of hydrate in accordance with the hydrate dissociation temperature which is around −11 °C for this concentration of NaCl (see Fig. 1).

On the basis of experimental results for varying salt concentration one can now propose the following schematic representation of the melting of ice and of formation followed by dissociation of hydrate in an emulsions containing CCl_3F (Fig. 10). So far it is assumed that only ice and salt are present in the droplets after the quenching of the emulsion in liquid nitrogen even though X rays data did not allow the identification of either anhydrous or hydrated solid form of NaCl in emulsion droplets. When such an emulsion is heated up to the eutectic temperatures of H_2O–NaCl system of −27 °C, water molecules liberated from crystal structure by melting of ice are captured in another solid structure of gas clathrate because the system is far from equilibrium represented by hydrate-NaCl solution equilibrium curve of Fig. 1. With respect to solid hydrate the solution is undercooled so that growth of hydrate crystals can go on until equilibrium for a given temperature is reached. By increasing the temperature of the sample further melting of ice takes place due to the presence of salt while the solution is still undercooled with respect to solid hydrate. Simultaneous crystallization of hydrate leads to complete dissociation of ice as represented on the right hand side of the phase diagram in Fig. 10. Since ice melting is absorbing heat while crystallisation of solid gas hydrate liberates heat, the total amount of exchanged energy can be very small (or even zero). Therefore calorimetry alone can not give a complete picture of the underlying phenomena, but combined with structural analysis it can furnish very precise picture as it was shown in this section.

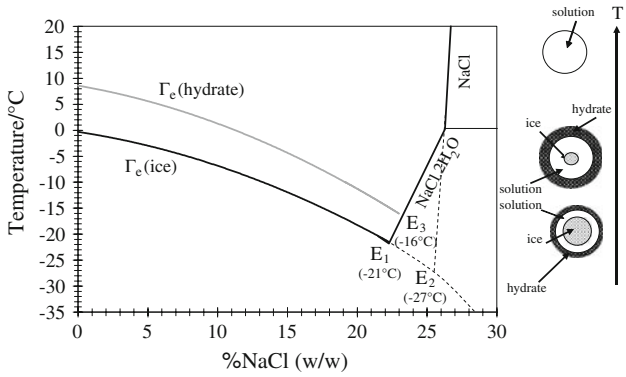

Fig. 10 Water–NaCl–CCl_3F pseudo-phase diagram and schematic representation of rapidly frozen water droplet composition change taking place during heating

Conclusions

From combined structural and calorimetric analysis of frozen water in oil emulsions containing variable concentration of NaCl in dispersed phase and hydrate forming species in continuous oil phase it was possible to show that ice, salt and hydrate show also some differences concerning their formation. Ice and salt are formed during the emulsion quenching while hydrate crystallizes throughout the progressive melting of ice caused by the regular heating of the frozen emulsion. Since the equilibrium temperature for ice and NaCl solution on one hand and hydrate and solution on the other hand is not the same, the droplets containing ice, hydrate and solution are not in equilibrium. Therefore ice melts while hydrate crystallizes in the remaining solution which is supersaturated with respect to hydrate. Initiation of such a process in gas and oil installations can provoke continuous crystallization of hydrate as long as ice is present in aqueous solution of NaCl. When all ice is melted, the system composed of hydrate and solution reaches equilibrium. During the subsequent heating progressive melting of hydrate is observed until the equilibrium point for the given concentration. The influence of the amount of salt upon hydrate dissociation and ice melting is similar and probably related to the affinity between water molecules and alkali halide ions. In order to precise the kinetic aspect of hydrate and ice formation and the competition of their formation studies at constant temperature are in progress in our laboratory.

Acknowledgements Constant interest for the subject and helpful discussions with Christine Dalmazzone of IFP and Didier Dalmazzone of ENSTA are gratefully acknowledged. Pierre Lesieur and Gerard Keller are acknowledged for help with LURE D22 line installation.

References

1. Giavarini C, Maccioni F, Santarelli ML. Modulated DSC for gas hydrates analysis. J Therm Anal Calorim. 2006;84(2):419–24.
2. Jakobsen T, Sjöblom J, Ruoff P. Kinetics of gas hydrate formation in W/O emulsions. The model system trichlorofluoromethane/water/non-ionic surfactant studied by means of dielectric spectroscopy. Colloids Surf. 1996;112:73–84.
3. Fouconnier B, Legrand V, Komunjer L, Clausse D, Bergflodt L, Sjöblom J. Formation of trichlorofluoromethane hydrate in w/o emulsions studied by differential scanning calorimetry. Prog Colloid Polym Sci. 1999;112:105–8.
4. Dalmazzone D, Clausse D, Dalmazzone C, Herzhaft B. The stability of methane hydrates in highly concentrated electrolyte solutions by differential scanning calorimetry and theoretical computation. Am Mineral. 2004;89(8–9):1183–91.
5. Dalmazzone D, Hamed N, Dalmazzone C, Rousseau L. Application of high pressure DSC to the kinetics of formation of methane hydrate in water-in-oil emulsion. J Therm Anal Calorim. 2006;85(2):361–8.
6. Bonnefoy O, Gruy F, Herri JM. Van der Waals interactions in systems involving gas hydrates. Fluid Phase Equilibria. 2005; 231(2):176–87.
7. Sinquin A, Palermo T, Peysson Y. Rheological and flow properties of gas hydrate suspensions. Oil Gas Sci Technol. 2004; 59(1):41–57.
8. Sloan ED. Clathrate hydrate of natural gases. New York: Marcel Dekker Inc.; 1990.
9. Barker JW, Gomez RK. Formation of hydrates during deepwater drilling operations. J Pet Technol. 1989;41:297–301.
10. Fouconnier B, Komunjer L, Ollivon M, Lesieur P, Keller G, Clausse D. Study of CCl_3F hydrate formation and dissociation in W/O emulsions by differential scanning calorimetry and X-ray diffraction. Fluid Phase Equilibria. 2006;250:76–82.
11. Clausse D, Babin L, Broto F, Aguerd M, Clausse M. Kinetics of ice nucleation in aqueous emulsions. J Phys Chem. 1983;87: 4030–4.
12. Franks F. Water—a comprehensive treatise, vol. 7. New York: Plenum; 1982.
13. Koop T, Luo B, Tsias A, Peter T. Water activity as the determinant for homogeneous ice nucleation in aqueous solutions. Nature. 2000;406:611–4.
14. Koop T, Bertram AK, Molina LT, Molina MJ. Phase transitions in aqueous NH_4HSO_4 solutions. J Phys Chem A. 1999;103:9042–8.
15. Fouconnier B, Manisol Y, Dalmazzone D, Clausse D. Study of trichloroflouromethane hydrate formation in w/o emulsions: dissociation energy and equilibria with salt-water solutions. Entropie. 2002;239/240:72–7.
16. Lopez C, Lesieur P, Bourgaux C, Keller G, Ollivon M. Thermal and structural behavior of milk fat. J Colloid Interface Sci. 2001;240:150–61.
17. Keller G, Lavigne F, Forte L, Andrieux A, Dahim M, Loisel C, et al. DSC and X-ray diffraction coupling: specifications and applications. J Therm Anal Calorim. 1998;51:783–91.
18. Lipkowski J. Hydrophobic hydratation; ecological aspects. J Therm Anal Calorim. 2006;83(3):525–31.
19. Herbstein FH. Crystalline molecular complexes and compounds; structure and principles. Oxford: Oxford University Press; 2005.
20. Udachin KA, Ratcliffe CI, Ripmeester JA. Single crystal diffraction studies of structures I, II et H hydrates: cage occupancy et composition. J Supramol Chem. 2002;2:405–8.
21. Belosludov VR, Inerbaev TM, Subbotin OS, Belosludov RV, Kudoh J, Kawazoe Y. Thermal expansion and lattice distortion of clathrate hydrates of cubic structures I and II. J Supramol Chem. 2002;2:453–8.
22. Davies SR, Hester KC, Lachance JW, Koh CA, Sloan ED. Studies of hydrate nucleation with high pressure differential scanning calorimetry. Chem Eng Sci. 2009;64:370–5.
23. Zhang Y, Debenedetti PG, Prud'homme RK, Pethica B. Differential scanning calorimetry studies of clathrate hydrate formation. J Phys Chem B. 2004;108:16717–22.
24. Clausse D. Thermal behaviour of emulsions studied by differential scanning calorimetry. J Therm Anal Calorim. 1998;51: 191–201.
25. Clausse D. Research techniques utilizing emulsions. Encyclopaedia of emulsion technology, chapter 2. New York: Marcel Dekker; 1983. p. 77–157.
26. Dalmazzone C, Clausse D. Microcalorimetry. Encyclopaedic handbook of emulsion technology, chapter 14. New York: Marcel Dekker; 2001. p. 327–41.
27. Clausse D, Babin L, Sifrini I, Broto F, Dumas JP. Nucleation of droplets of aqueous solutions of NH_4Cl or NaCl. Water and steam—their properties and current industrial applications. Oxford and New York: Pergamon Press; 1980. p. 664–71.
28. Kanno H, Angel CA. Homogeneous nucleation and glass formation in aqueous alkali halide solutions at high pressures. J Chem Phys. 1977;81(26):2639–43.
29. Sassi O, Sifrini I, Dumas JP, Clausse D. Theoretical curves in thermal analysis for the melting of binaries showing solid solution. Phase Transit. 1988;13:101–11.